1,2,a)   1,b)   2,c)

Non-negative Matrix

Factorization　NMF

1   2

NMF

,   ,

Estimating Lighting and Geometry Information
from Time-Lapse Videos via Non-Negative Matrix Factorization

Bing-Yu Chen[1,2,a]   Hsin-Yi Chen[1,b]   Tomoyuki Nishita[2,c]

Abstract: To create appealing realistic visual effects, complete geometric models, lightings, and material properties of a scene are often required in film production or augmented reality. This compact representation also enables various applications in many image synthesis and editing tasks. In this paper, we introduce an iterative photometric stereo approach via non-negative matrix factorization (NMF) to model an outdoor scene from a time-lapse video, and retrieve the surface geometry and lighting information of the scene even in the presence of shadow. To accomplish this, in this paper, we provide 1) a novel shadow detection method to locate shadow pixels in a time-lapse video, and 2) an iterative photometric stereo framework with NMF to recover the geometry and lighting information of the outdoor scene.

Keywords: image decomposition, time-lapse video, non-negative matrix factorization

1. Introduction

The goal of realistic image synthesis is to produce computer-generated images that are indistinguishable from real photographs. The process needs detailed models of scenes including light sources and objects specified by their geometry and material properties. One of the best ways of obtaining these data is through the measurements of the scene attributes from real photographs by inverse rendering. However, classic inverse rendering methods have been largely limited to the settings with highly controlled lightings or known geometry. Hence, many of them only focused on small objects or indoor scenes. Even for the methods that worked in outdoor environments, they are usually based on some special setups to record the illuminations during the scene capturing. As well, they required the prerequisite of the surface geome-

1　National Taiwan University
2　The University of Tokyo
a)　robin@ntu.edu.tw
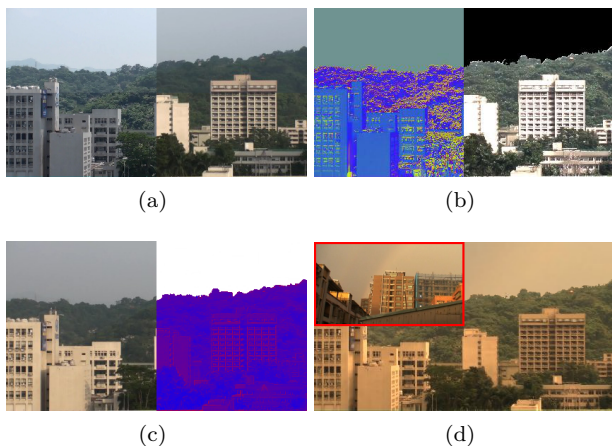b)　fensi@cmlab.csie.ntu.edu.tw
c)　nis@is.s.u-tokyo.ac.jp

1 (a) Four frames of the input time-lapse video. (b) The extracted normal map (left) and reflectance map (right). (c) The synthesized image (left) and the difference image (right) by comparing with its original input image. In the difference image, the blue color indicates small difference, while the red color indicates large difference. (d) The lighting transfer result. The small figure on the left-upper side is the source image, and its extracted lighting parameters are applied to the target scene.

try. Although there are many techniques available for 3D building reconstruction and surface reflectance measurement, it is well-known that acquiring such information is extremely difficult, especially in complicated and diverse outdoor scenes.

An alternative line of inverse rendering utilized time-lapse data to recover various scene properties including scene geometry, surface reflectance, shadows, illuminations, and camera parameters. The major advantage of the time-lapse data is that, by observing the same scene under many different lighting conditions, it contains much more information that can be extracted comparing to using either a single image or an unstructured video via dense sampling. Several previous works have explored this data source. Lalonde *et al.* [6] estimated the illumination model by using the time-lapse data. Thereby, it enables to illumination-consistent appearance transfer across different cameras. However, their method requires complicated preprocessing and camera location, thus it cannot be applied on image sequences obtained from general sources, for example on-line videos. Closely related to our method is that of Sunkavalli *et al.* [16]. They decomposed the scene into shadow, illumination, and reflectance components under some assumptions on the distribution of the shadow and sky condition. Since they only recovered a partial geometry of the scene, their factored representation cannot be transferred to another scene directly. In contrast, our goal is to extract both the surface geometry

and lighting properties of the scene without the requirement of knowing the camera location, shadow distribution, and weather condition.

Therefore, we introduce an iterative photometric stereo approach with non-negative matrix factorization (NMF) to model an outdoor scene from a time-lapse video, and retrieve the surface geometry and lighting information even in the presence of shadow.

2. Related Work

Inverse Rendering. Inverse rendering refers to recover from real photographs the attributes of scenes, including reflectance, lightings, and textures. Ramamoorthi and Hanrahan [12] presented a signal-processing framework of reflection, which is useful in theoretical analysis and various practical applications of inverse rendering. For indoor setting, there are a significant amount of methods [3], [13], [15], which produced high quality measurements and leading to the creation of realistic images. There are also some methods designed for outdoor environments under natural illumination. Assuming a simple parametric model for skylight, Yu and Malik [20] proposed to solve a series of optimization problems to find the parameters of appropriate lighting and reflectance models. Debevec *et al.* [4] estimated the reflectance properties of the surfaces via iterative optimization. Similarly, Nimeroff *et al.* [11] rendered scenes under natural illumination by combining several basis images.

Time-Lapse Sequence Analysis. Intrinsic images [1] are mid-level description of a scene. An image can be decomposed into two intrinsic images: a reflectance image and an illumination image. Although decomposing a single image into the intrinsic images remains a difficult problem, deriving intrinsic images from an image sequence has seen great success. Weiss [18] used a maximum likelihood framework to recover the intrinsic images from a time-lapse video in which the illumination varies but the reflectance remains constant. Matusik *et al.* [10] used time-lapse data to estimate the reflectance field for a fixed viewpoint by solving an optimization problem, but a light probe camera is needed to estimate the incident illumination. Lalonde *et al.* [6] proposed to use time-lapse data with GPS information to geometrically calibrate the camera position. Sunkavalli *et al.* [16] described a method for converting a time-lapse video of an outdoor scene into the basis curves where the data at each pixel has been factored into illumination, geometry, and reflectance components. Besides, there is also some recent work focused

on the problem of analyzing and extracting information from time-lapse video sequence, e.g. [7][17].

Photometric Stereo. Woodham [19] introduced photometric stereo, which is a method allows us to recover the surface normal and reflectance of Lambertian objects from a set of images obtained under several different lighting conditions by solving a linear system. Hayakawa [5] presented an unconstrained photometric method using SVD to estimate the surface normal and reflectance of objects without a prior knowledge of the light-source direction and intensity. Yullie *et al.* [21] extended this method to a rank-4 formulation that allows to recover the ambient light but assumed all images share a common background ambient lighting. Photometric stereo under complex illumination has also been demonstrated in [2]. Recently, applications of photometric stereo are also proposed. For example, Shen *et al.* [14] extend photometric stereo method to do weather estimation.

3. Background

Lambertian Surface Model. In many works, to overcome the high dimensionality of BRDF (Bidirectional Reflectance Distribution Function) and make the recovering process feasible, more compact representations depended on a small number of parameters have been developed. The simplest reflectance model used in many problems is Lambertian reflectance model. We assume that the surface point $(x, y, Z(x, y))$ with the normal direction $N(x, y)$ on the pixel (x, y) of a captured image is illuminated by a distant light-source whose direction is denoted by vector M. We also assume that the surface point absorbs the incoming light of various wavelengths $c \in \{r, g, b\}$ according to the reflectance function $\rho(x, y)$. Under the Lambertian reflection model, a pixel intensity $i^c(x, y)$ in the captured image is given by

$$i^c(x, y) = \rho^c(x, y)[N(x, y) \cdot M^c]. \tag{1}$$

Photometric Stereo. In calibrated photometric stereo techniques, the problem is to derive the surface normal, surface reflectance, light-source direction, and light-source intensity simultaneously. The formulation of photometric stereo is described as follows: a measurement matrix $\mathbf{I}$ contains the intensities of P pixels through F frames. Assuming that the surface follows the Lambertian reflectance model, this measurement matrix can be factorized as:

$$\mathbf{I} = \mathbf{RNMT},$$

where $\mathbf{R}_{P \times P}$ is the surface reflectance $P \times P$ diagonal matrix and only the diagonal elements contain the reflectance

values, $\mathbf{N}_{P \times 3}$ is the surface normal $P \times 3$ matrix, $\mathbf{M}_{3 \times F}$ is the light-source direction $3 \times F$ matrix, and $\mathbf{T}_{F \times F}$ is the light-source intensity $F \times F$ diagonal matrix. Therefore, from the multiple images captured by a fixed camera under varying illuminations, the surface model can be formulated as :

$$\mathbf{I} = (\mathbf{RN})(\mathbf{MT}) = \mathbf{SL},$$

where $\mathbf{S} = \mathbf{RN}$, $\mathbf{L} = \mathbf{MT}$, each row of $\mathbf{S}$ encodes the reflectance and orientation of a scene point, and each column of $\mathbf{L}$ encodes the direction and intensity of the light-source. Traditionally, SVD is usually applied to derive both $\mathbf{L}$ and $\mathbf{S}$, i.e., $\mathbf{I} \approx \hat{\mathbf{S}}\hat{\mathbf{L}}$, where $\hat{\mathbf{S}}$ and $\hat{\mathbf{L}}$ are the factorized results representing surface geometry and light direction. However, because shape reconstruction is the main concern in the photometric stereo problem, using SVD to reconstruct the surface normal also limit the estimated albedo and light magnitude to be gray-level.

Matrix Factorization using NMF. Although SVD is a well-known method for matrix factorization, in some situations there also some limitations of SVD. For example, it cannot be directly applied to the intensity matrix with missing data. As well, the factorized basis vectors may contain both positive and negative components, but the negative components may contradict to the physical realities in our factorization process. Thus, we propose to use NMF [8], [9] to deal with the missing data and search for the non-negative vectors as the representative basis. NMF can be formulated as follows: given an $n \times m$ matrix $\mathbf{V}_{n \times m}$ with each element $v_{ij} \geq 0 \in \mathbf{V}$ and a prespecified positive integer $r < min(n, m)$, NMF can find two non-negative matrices $\mathbf{W}$ and $\mathbf{H}$, such that $\mathbf{V} \simeq \mathbf{WH}$, where their elements $w_{ij} \geq 0 \in \mathbf{W}$ and $h_{ij} \geq 0 \in \mathbf{H}$. If each column of $\mathbf{V}$ represents an object, NMF approximates it by a linear combination of r "basis" columns in $\mathbf{W}$. The conventional approach to find $\mathbf{W}$ and $\mathbf{H}$ is by minimizing the difference between $\mathbf{V}$ and $\mathbf{WH}$.

4. Geometry and Lighting Extraction

For an image sequence, where a surface point is lit by different light sources in different frames, Eq. (1) can be extended as:

$$i_k^c(x, y) = \rho^c(x, y)[N(x, y) \cdot M_k^c], \tag{2}$$

where $k = 1, 2, ..., F$ is the image index and F is the number of images. There are two important assumptions in this model: the surface points 1) are lit by the same distance light source, and 2) are not in the shadow of any

light source. This illumination model is suitable for indoor object(s), since we can control the lightings to prevent the shadow. However, in an outdoor environment, the above assumptions are usually violated:

(1) The sunlight itself only affects the scene in some parts as the sun is a directional light source, but the skylight scatters around a large portion of the outdoor scene and influences the scene with indirect illumination.

(2) Under the orthographic projection, the only light source direction that can result in an entirely shadowless image, is the one aligned with the viewing direction. Consequently, shadowing is inevitable in an outdoor time-lapse video since the light source moves but the viewing direction is fixed.

Therefore, we first detect the shadow pixels (Section 4.2) to ignore them in the factorization process, and then perform the rest factorization processes (Sections 4.3 and 4.4). In addition, our model assumes that the color of visible pixels is due to the reflection from the surfaces in the scene. Hence, we do not consider the sky pixels in our representation, and those pixels are removed in advance.

4.1 Problem Formulation

For modeling the sky light in a real scene, we include an ambient term $a_k^c(x, y)$ into the illumination model in Eq. (2):

$$i_k^c(x, y) = \rho^c(x, y)[N(x, y) \cdot M_k^c + a_k^c(x, y)]. \tag{3}$$

The above equation is formulated for one pixel (x, y) on one frame k. When there are F frames and every frame contains P pixels, we will have $P \times F$ equations, which can be written into a matrix form with a rank-4 formulation:

$$\mathbf{I}^c = (\mathbf{R}^c \mathbf{N})(\mathbf{M} \mathbf{T}^c) = \mathbf{S}^c \mathbf{L}^c, \tag{4}$$

where $\mathbf{I}_{P \times F}$ is the stack of the intensities of all pixels in all frames, $\mathbf{S}_{P \times 4}$ encodes the reflectance $\mathbf{R}$ and orientation $\mathbf{N}$ of each surface point, and $\mathbf{L}_{4 \times F}$ encodes the directions $\mathbf{M}$ and spectra $\mathbf{T}$ of the light sources.

Besides, we observed that the establishment of Eq. (4) does not always hold, because some values (pixels) in $\mathbf{I}^c$ might be shadowed in some frames. Hence, we include a shadow mask $\mathbf{C}$ into Eq. (4). Then, the illumination model in the matrix formulation becomes:

$$\mathbf{C} \circ \mathbf{I}^c = \mathbf{C} \circ (\mathbf{S}^c \mathbf{L}^c) = \mathbf{C} \circ (\mathbf{R}^c \mathbf{N} \mathbf{M} \mathbf{T}^c), \tag{5}$$
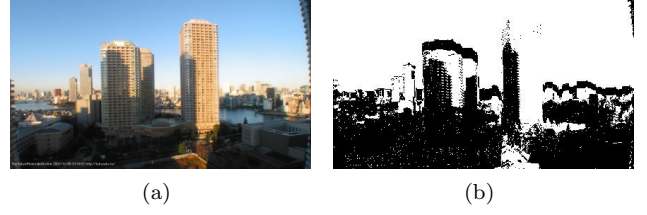

2 An example of shadow detection. (a) The original image captured by a webcam. (b) The detected shadow map of (a). The shadow is indicated by black color.

where $\circ$ denotes an element-wise matrix multiplication, and $c_{i,j} = 0 \in \mathbf{C}$ indicates a shadow pixel; otherwise $c_{i,j} = 1$.

Consequently, our problem is converted to an inverse problem in a matrix form: given an measurement matrix $\mathbf{I}^c \geq 0$ in the Lambertian surface reflectance model, the question is to decide the surface geometry and lighting parameters $\mathbf{R}^c$, $\mathbf{T}^c$, $\mathbf{N}$, $\mathbf{M}$, and the confidence matrix $\mathbf{C}$, while satisfying the following constraints:

(1) $\mathbf{N} \times \mathbf{N} \geq 0$, for the non-shadow pixels;

(2) $\mathbf{R}^c \geq 0$;

(3) $\mathbf{T}^c \geq 0$.

To tackle this problem, we first propose a shadow detection method to estimate the shadow matrix $\mathbf{C}$. Then, we introduce an iterative two-stage factorization framework to estimate $\mathbf{R}^c$, $\mathbf{N}$, $\mathbf{M}$, and $\mathbf{T}^c$.

4.2 Shadow Detection

The illumination model described in Eq. (4) assumes that every pixel in the same scene receives the same light. However, if a pixel is in shadow, its illumination should not be equal to that of other pixels in the same scene. Hence, if we pretend that a shadowed pixel receiving the same light as the other pixels, the estimated albedo for this pixel should be smaller than its actual value. Therefore, we first try to estimate the actual albedo $\rho(p)$ for each surface point p. We assumed that every surface point is not in shadow in at least four frames. Hence, the actual albedo $\rho(p)$ is estimated by the estimated initial light $\mathbf{L}$ and the intensity values $\mathbf{I}_4(p)$ from four shadow-less frames. After that, we use the initial light $\mathbf{L}$ to compute the per-frame albedo $\tilde{\rho}_k(p)$ for each pixel p in each frame k. Finally, if the computed per-frame albedo $\tilde{\rho}_k(p)$ in the frame is smaller than the actual albedo $\rho(p)$, we conclude that this pixel p is the shadow in this frame. The following procedures are performed to construct a shadow mask $\mathbf{C}_k \in \mathbf{C}$ for each frame k.

4.2.1 Initial Light Estimation

To estimate the initial light $\mathbf{L}_k \in \mathbf{L}$ of the scene in each frame k, we factorize the grey-level intensity matrix $\mathbf{I}$ by adopting the projected gradient NMF [9]: $\mathbf{I} \approx \mathbf{SL}$. Formally, NMF decomposes a $P \times F$ data matrix $\mathbf{I}$ into the product of a $P \times R$ surface matrix $\mathbf{S}$ and a $R \times F$ lighting matrix $\mathbf{L}$, where P is the number of pixels in one image and F is the number of images. The algorithm takes the basis dimension R as the input. Setting R to different values means using different dimensions of basis to represent the original data. Since we assume that the surface illumination are from the sun light and sky light, we set $R = 4$ for the decomposition process. After the factorization, we derive an estimated lighting matrix $\mathbf{L}$ as the initial light.

4.2.2 Shadow Identification

In the following steps, we show the procedures to identify the shadow pixels in each frame.

(1) For each frame, we first assign every pixel a rank of position in the current frame according to its brightness. The pixel has lower rank if it is brighter, and vise versa. Then, for each surface point p, we find the first 4 frames that their corresponding pixels p have the lowest ranks. The derived frame indexes for the surface point p are denoted as: $[k_1, k_2, k_3, k_4]_p$, where $k_{1,...4} = 1, 2, ...F$.

(2) For each surface point p, we use the intensity data collected from the shadow-less frames selected in Step 1. and the initial light $\mathbf{L}$ estimated in Section 4.2.1 to estimate the actual albedo $\rho(p)$ of the surface point p by solving the following equations:

$$\mathbf{I}_4(p) = [i_{k_1}(p), i_{k_2}(p), i_{k_3}(p), i_{k_4}(p)] = \mathbf{S}(p) \cdot \mathbf{L},$$

$$\rho(p) = \parallel \mathbf{S}(p) \parallel_2 .$$

Then, for each pixel p, we calculate its per-frame albedo $\tilde{\rho}_k(p)$ for each frame k by solving the following equation:

$$i_k(p) = \tilde{\rho}_k(p) \cdot \mathbf{L}_k.$$

(3) For each pixel p, we compare its per-frame albedo $\tilde{\rho}_k(p)$ with the estimated actual albedo $\rho(p)$. If the distance between these two values is greater than a certain threshold, we mark the pixel p in the frame k as in the shadow.

2 (b) shows the detected shadow mask of 2 (a), which is captured by a webcam.

4.3 First Factorization

The objective of the first factorization is to estimate the

(a)   (b)

3 An example of normal extraction. (a) The original captured image. (b) The extracted normal map of (a).

surface normal $\mathbf{N}$ and the light direction $\mathbf{M}$ in Eq. (5), where $\mathbf{I}^c$ is given and $\mathbf{C}$ is estimated in the previous section. To exclude the influence of the shadowed pixels, we extend the projected gradient NMF method originally proposed in [9]. By incorporating the shadow mask $\mathbf{C}$ into the NMF objective function, we can weight the contribution of each element in $\mathbf{I}^c$ toward the error. Setting an entry of $\mathbf{C}$ to zero will cause the corresponding measurement to have no effect on the factorization error. Accordingly, the new objective function is formulated as :

$$\sum_{i,j} (c_{i,j} \circ (\mathbf{I} - \mathbf{SL})_{i,j})^2,$$

where $(\mathbf{I} - \mathbf{SL})_{i,j}$ is one of the elements of the matrix $(\mathbf{I} - \mathbf{SL})$.

Thereby, NMF is applied. To be more robust, we used the derived lighting matrix $\mathbf{L}^c$ to re-estimate the shadow mask $\mathbf{C}$ again by the same approach described in Section 4.2.2. Then, we use the refined shadow map $\mathbf{C}$ to re-estimate the surface matrix $\mathbf{S}^c$ and the lighting matrix $\mathbf{L}^c$. The above processes can be performed iteratively. After obtaining the refined surface matrix $\mathbf{S}^c$ and lighting matrix $\mathbf{L}^c$, the normal matrix $\mathbf{N}$ and the light direction matrix $\mathbf{M}$ are derived as:

$$\mathbf{N} = \frac{\mathbf{S}}{\parallel \mathbf{S} \parallel}, \mathbf{M} = \frac{\mathbf{L}}{\parallel \mathbf{L} \parallel}.$$

3 (b) shows the extracted normal map of 3 (a).

4.4 Second Factorization

Once the surface normal $\mathbf{N}$ and the light direction $\mathbf{M}$ in Eq. (5) are estimated in Section 4.3, the remainder now are the surface albedo matrix $\mathbf{R}^c$ and the light intensity matrix $\mathbf{T}^c$.

Surface Albedo Estimation. By setting a matrix $\mathbf{V}^c = \mathbf{C} \circ (\mathbf{I}^c \oslash \mathbf{N M})$, we can approximate $\mathbf{R}^c$ and $\mathbf{T}^c$ by factorizing $\mathbf{V}^c$, where $\oslash$ denotes the element-wise matrix division. In the revised NMF method, the confidence term is set as 0 when the inner product $\mathbf{N M}$ is less than 0 or bigger than 1, because the cosine term could not be larger than 1 or less than 0. In addition, we only keep the estimated albedo matrix $\mathbf{R}^c$ in this stage, since the estimated
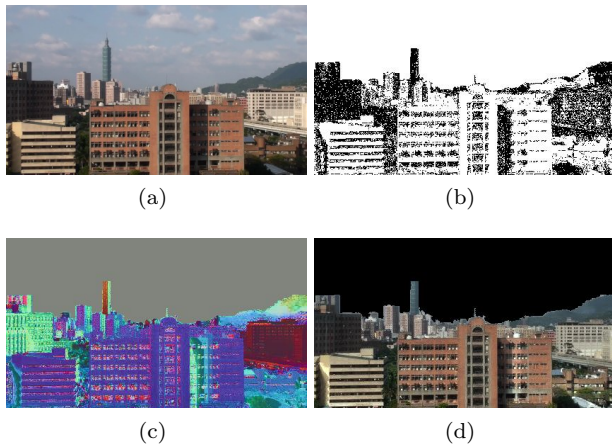
4 Factorization results. (a) The original captured image. (b) After removing sky and detecting shadow. (c) The extracted normal map. (d) The extracted reflectance map.

$\mathbf{T}^c$ is not so reliable in this factorization process.

Light Intensity Estimation. Until this stage, the last unknown is the light intensity matrix $\mathbf{T}^c$ which can be simply solved by the least squares estimation.

5. Result

1 and 4 show some extraction results. 1 (b) and 4 (c) (d) show the extracted normal maps and reflectance maps of 1 (a) and 4 (a), respectively.

4 (b) also show the image after removing the sky and detecting the shadow, where the shadow is indicated by black color.

6. Conclusion

Recovering all intrinsic properties, such as lighting, geometry, and materials of a physical-based appearance model is difficult when all of them are unknown. While this problem is ill-posed in nature, we have presented a new technique for determining the geometry and lighting information of the entire scene. The key insight is to extend the classical photometric stereo approach to model complex outdoor scenes. We propose an iterative NMF framework to decompose a time-lapse video into the geometry term and the lighting term in the presence of shadow. One strength of our approach is that no assumption are placed on the time-lapse video, so we can flexibly apply our method on various sources with general conditions.

[1] Barrow, H. G. and Tenenbaum, J. M.: Recovering intrinsic scene characteristics from images, *Computer Vision Systems*, Academic Press, pp. 3–26 (1978).

[2] Basri, R., Jacobs, D. and Kemelmacher, I.: Photometric Stereo with General,Unknown Lighting, *IJCV*, Vol. 72, No. 3, pp. 239–257 (2007).

[3] Debevec, P., Hawkins, T., Tchou, C., Duiker, H.-P., Sarokin, W. and Sagar, M.: Acquiring the Reflectance Field of a Human Face, *Proc. SIGGRAPH '00*, pp. 145–156 (2000).

[4] Debevec, P., Tchou, C., Gardner, A., Hawkins, T., Poullis, C., Stumpfel, J., Jones, A., Yun, N., Einarsson, P., Lundgren, T., Fajardo, M. and Martinez, P.: Estimating Surface Reflectance Properties of a Complex Scene under Captured Natural Illumination, Technical Report ICT-TR-06.2004, USC (2004).

[5] Hayakawa, H.: Photometric Stereo under a Light Source with Arbitrary Motion, *JOSA*, Vol. 11, No. 11, pp. 3079–3089 (1994).

[6] Lalonde, J.-F., Efros, A. A. and Narasimhan, S. G.: Webcam clip art: appearance and illuminant transfer from time-lapse sequences, *TOG*, Vol. 28, No. 5, pp. 131:1–131:10 (2009).

[7] Lalonde, J.-F., Narasimhan, S. G. and Efros, A. A.: What do the sun and the sky tell us about the camera?, *IJCV*, Vol. 88, No. 1, pp. 24–51 (2010).

[8] Lee, D. D. and Seung, H. S.: Algorithms for Nonnegative Matrix Factorization, *Proc. NIPS '00*, pp. 556–562 (2000).

[9] Lin, C.-J.: Projected Gradient Methods for Nonnegative Matrix Factorization, *Neural Comput.*, Vol. 19, No. 10, pp. 2756–2779 (2007).

[10] Matusik, W., Loper, M. and Pfister, H.: Progressively-Refined Reflectance Functions from Natural Illumination, *Proc. EGSR '04*, pp. 299–308 (2004).

[11] Nimeroff, J., Simoncelli, E. and Dorsey, J.: Efficient Re-Rendering of Naturally Illuminated Environments, *Proc. EGWR '94*, pp. 359–373 (1994).

[12] Ramamoorthi, R. and Hanrahan, P.: A Signal-Processing Framework for Inverse Rendering, *Proc. SIGGRAPH '01*, pp. 117–128 (2001).

[13] Sato, Y., Wheeler, M. D. and Ikeuchi, K.: Object Shape and Reflectance Modeling from Observation, *Proc. SIGGRAPH '97*, pp. 379–388 (1997).

[14] Shen, L. and Tan, P.: Photometric stereo and weather estimation using internet images, *Proc. CVPR '09*, pp. 1850–1857 (2009).

[15] Stephen R. Marschner, Stephen H. Westin, E. P. L. K. E. T. and Greenberg, D. P.: Image-Based BRDF measurement, *Applied Optics*, Vol. 39, No. 16, pp. 2592–2600.

[16] Sunkavalli, K., Matusik, W., Pfister, H. and Rusinkiewiez, S.: Factored Time-Lapse Video, *TOG*, No. 3, pp. 101:1–101:10 (2007).

[17] Sunkavalli, K., Romeiro, F., Matusik, W., Zickler, T. and Pfister, H.: What do color changes reveal about an outdoor scene?, *Proc. CVPR '08* (2008).

[18] Weiss, Y.: Deriving intrinsic images from image sequences, *Proc. ICCV '01*, Vol. 2, pp. 68–75 (2001).

[19] Woodham, R. J.: Photometric Method for Determining Surface Orientation from Multiple images, *Optical Eng.*, Vol. 19, No. 1, pp. 139–144 (1980).

[20] Yu, Y. and Malik, J.: Recovering Photometric Properties of Architectural Scenes from Photographs, *Proc. SIGGRAPH '98*, pp. 207–218 (1998).

[21] Yullie, A. L., Snow, D., Epstein, R. and Belhumeur, P. N.: Determining Generative Models of Objects under Varying Illumination: Shape and Albedo from Multiple Image using SVD and Integrability, *IJCV*, Vol. 35, No. 3, pp. 203–222 (1999).